Evol Biol
DOI 10.1007/s11692-008-9038-3

RESEARCH ARTICLE

The Evolution of Modularity in the Mammalian Skull I: Morphological Integration Patterns and Magnitudes

Arthur Porto · Felipe B. de Oliveira · Leila T. Shirai · Valderes De Conto · Gabriel Marroig

Received: 30 June 2008 / Accepted: 12 September 2008

Abstract Morphological integration refers to the modular structuring of inter-trait relationships in an organism, which could bias the direction and rate of morphological change, either constraining or facilitating evolution along certain dimensions of the morphospace. Therefore, the description of patterns and magnitudes of morphological integration and the analysis of their evolutionary consequences are central to understand the evolution of complex traits. Here we analyze morphological integration in the skull of several mammalian orders, addressing the following questions: are there common patterns of inter-trait relationships? Are these patterns compatible with hypotheses based on shared development and function? Do morphological integration patterns and magnitudes vary in the same way across groups? We digitized more than 3,500 specimens spanning 15 mammalian orders, estimated the correspondent pooled within-group correlation and variance/covariance matrices for 35 skull traits and compared those matrices among the orders. We also compared observed patterns of integration to theoretical expectations based on common development and function. Our results point to a largely shared pattern of inter-trait correlations, implying that mammalian skull diversity has been produced upon a common covariance structure that remained similar for at least 65 million years. Comparisons with a rodent genetic variance/covariance matrix suggest that this broad similarity extends also to the genetic factors underlying phenotypic variation. In contrast to the relative constancy of inter-trait correlation/covariance patterns, magnitudes varied markedly across groups. Several morphological modules hypothesized from shared development and function were detected in the mammalian taxa studied. Our data provide evidence that mammalian skull evolution can be viewed as a history of inter-module parcellation, with the modules themselves being more clearly marked in those lineages with lower overall magnitude of integration. The implication of these findings is that the main evolutionary trend in the mammalian skull was one of decreasing the constraints to evolution by promoting a more modular architecture.

Keywords Constraints · Genetic architecture · Selection · Development · Phenotypic and genetic covariance

A. Porto · F. B. de Oliveira · L. T. Shirai · V. De Conto · G. Marroig (✉)
Laboratório de Evolução de Mamíferos, Departamento de Genética e Biologia Evolutiva, Instituto de Biociências, Universidade de São Paulo, CP 11.461, CEP 05508-090 Sao Paulo, SP, Brasil
e-mail: gmarroig@usp.br

Introduction

Morphological integration refers to the relationships and connections among morphological elements (Olson and Miller 1958; Berg 1960; Chernoff and Magwene 1999). Empirically, morphological integration is recognized by detecting the existence of discrete groups of highly correlated traits, termed modules (or "correlation pleiades" sensu Berg 1960). The modular organization already observed in a variety of organisms has been claimed to be the outcome of functional and/or developmental relationships between traits (Olson and Miller 1958; Berg 1960); in other words, traits related by ontogeny or function have greater influence on each other than on those without shared function or developmental origin/interaction. Considering that traits in the same module usually share a common genetic basis (Cheverud 1982, 1984; Chernoff

and Magwene 1999), they are expected to evolve as an integrated unit (Lande 1979), providing a different perspective to investigate morphological evolution than studying individual traits. To quantify and compare modularity among groups, two complementary aspects of the morphological integration should be analyzed conjointly: pattern and magnitude (Marroig and Cheverud 2001). In this context, patterns of integration refer to the relationships between morphological elements and can be assessed by examining the correlation or covariance among traits. The magnitude of integration refers to the level or intensity of these associations between traits.

From a genetic perspective, morphological integration is the product of the so called genetic architecture (Falconer and Mackay 1996), a term used as a shortcut to the number of genes underlying the phenotypes observed, the distribution of the magnitude of its phenotypic effects and type of effect (additive, dominance, epistasis) and especially, since we are talking about correlation among traits, of pleiotropy and linkage disequilibrium. Usually, the emphasis in the quantitative genetics literature is placed on correlation between traits being produced by pleiotropy (Cheverud et al. 2004), because linkage disequilibrium is usually thought to be transient (unless actively maintained by selection) due to recombination among loci. Recent studies of genetic architecture in many organisms, and especially in mammals, have found ample evidence of a modular organization with pleiotropic effects usually falling within phenotypic modules and being reduced among modules (Ehrich et al. 2003; Cheverud et al. 2004; Wagner et al. 2008; Kenney-Hunt et al. 2008). Accordingly, a prerequisite for the evolution of modularity is that pleiotropy must be genetically variable. One mechanism by which genetic variation in pleiotropy can be achieved is by means of differential epistasis (Cheverud et al. 2004; Pavlicev et al. 2008). Notice that differential epistasis in pleiotropic effects can produce changes in both morphological integration patterns and magnitudes.

Among the evolutionary implications of such modular organization, two are particularly emphasized in the literature: (1) the high intercorrelation among traits from the same functional/developmental complex ensures the coordinated evolution of different parts of the organism while maintaining its cohesion/functionality (Klingenberg 2004); (2) the low (or absent) correlation among traits from different functional/developmental complexes permits them to evolve in a quasi-independent fashion, therefore, allowing the adaptation to different functions with little or no interference with other functions (Wagner et al. 2007). However, regardless of whether the emphasis is placed on the integration of parts into a coherent structure or their ability to vary independently, one of the main questions that should be asked is: why and to what degree is the variation of parts coordinated? A completely integrated structure would not allow any evolutionary flexibility, while a completely parcellated cranium, in which every trait behaves as an independent module, would fail to respond to evolutionary processes (e.g. selection) in a coordinated manner.

In this context, some fundamental questions should be addressed: (1) what are the pattern and magnitude of interactions among morphological traits? (2) how do patterns of intertrait relationships change through time? In particular, this last question, concerning the study of the evolution of integration patterns, remains a significant challenge to be addressed by evolutionary biologists. Theoretical studies have shown that integration patterns can evolve considerably fast (e.g., Pavlicev et al. 2008), while empirical investigations have provided inconclusive results. Several studies have shown that integration patterns remain considerably similar across species or higher taxonomic levels (e.g., Cheverud 1996; Ackermann and Cheverud 2000; Marroig and Cheverud 2001; Gonzalez-Jose et al. 2004; Preston and Ackerly 2004; Young and Badyaev 2006), but there is also evidence that strong selection can override and modify existing patterns of integration among traits (e.g., Beldade and Brakefield 2003).

The mammalian cranium is a particularly suitable structure to address these questions, since homologous cranial bones interact to cover the head organs and take part in various functions among diverse orders (Cheverud 1982, 1995). Moreover, common patterns of skull development have been found even among distant groups, providing a good opportunity to conduct comparative studies in an inclusive evolutionary context (Moore 1981; Smith 1997). Although the importance of broad comparative analyses has long been recognized (Chernoff and Magwene 1999; Eble 2004), few studies to date have presented data above the genus level (e.g., Cheverud 1989; Marroig and Cheverud 2001; Ackermann and Cheverud 2004).

Our approach here is to explore morphological integration in the mammalian skull in a broad phylogenetic framework. We sampled 15 mammalian orders to obtain a representative dataset on the diversity of integration patterns existent in this group. By examining overall similarity in phenotypic covariance/correlation patterns across orders, we evaluated the stability of modularity patterns throughout mammalian phylogenetic history. In order to assess if these patterns extended to the genetic factors underlying skull traits, we compared phenotypic data to an empirically determined genetic variance-covariance matrix (G-matrix). We also used theoretical connectivity matrices derived from functional/developmental hypotheses of morphological integration to

determine whether observed inter-trait relationship patterns mirrored predicted trait associations. Furthermore, the comparisons between theoretical and observed modularity allow us to access whether our sample of mammalian diversity differs in integration patterns. Finally, we calculate a morphological integration index that reflects the magnitude of the overall correlation between cranial traits. This information is complementary to correlation/covariance patterns, and helps to build a broader canvas against which the evolution of modularity structure in mammals can be analyzed.

Materials and Methods

Samples

A total of 3,644 skulls, representing 15 mammalian orders, were measured in this study. Only adult specimens with completely erupted and functional dentition, as well as basioccipital synchondrosis, were measured. One species or genus was chosen to represent each order, except for primates, in which seven genera, including *Homo*, were examined to provide a more detailed perspective. Table 1 presents the taxa sampled and the respective number of specimens analyzed. The taxonomic arrangement used throughout this study follows Wilson and Reeder (2005). Measured specimens were deposited in the following institutions: American Museum of Natural History (AMNH, New York), Anthropologisches Institut und Museum Zürich Universität (AIM, Zürich), Field Museum of Natural History (FMNH, Chicago), Museu de Anatomia Professor Alfonso Bovero (São Paulo), Museu de Anatomia Humana da Universidade Federal de São Paulo (São Paulo), Museu de Zoologia da Universidade de São Paulo (MZUSP, São Paulo), Museu Nacional da Universidade Federal do Rio de Janeiro (MNRJ, Rio de Janeiro), Museu Paraense Emílio Goeldi (MPEG, Belém), Museum National d'Histoire Naturelle (MNHN, Paris), Museum für Naturkunde (ZMB, Berlin), Museum of Vertebrate Zoology (MVZ, Berkeley), Museum of Comparative Zoology Harvard University (MCZ, Cambridge), Nationaal Natuurhistorisch Museum (RMNH, Leiden), Natural History Museum (BNHM, London), Smithsonian National Museum of Natural History (NMNH, Washington DC), Powell-Cotton Museum (PCM, Birchington-on-Sea), Royal Belgian Institute for the Natural Sciences (RBINS, Brussels), and Royal Museum for Central Africa (RMCA, Tervuren). A complete list of examined specimens is available from the authors upon request.

Table 1 List of taxa used as representatives of the 15 mammalian orders surveyed in this study, with the respective sample size

Infraclass	Order	Genus/species	Sample size	Controlled variation
Metatheria	Didelphimorphia	*Didelphis*	215	S, SP, SxSP
	Paucituberculata	*Caenolestes*	60	S, G
	Dasyuromorphia	*Antechinus leo*	53	–
	Diprotodontia	*Macropus robustus*	60	SSP
	Peramelimorphia	*Isodon macrourus*	59	SSP
Eutheria	Hyracoidea	*Procavia capensis*	45	SSP
	Macroscelidea	*Elephantulus brachyrhynchus*	57	–
	Cingulata	*Dasypus novemcinctus*	60	G
	Scandentia	*Tupaia glis*	60	SSP, SxSSP
	Lagomorpha	*Sylvilagus brasiliensis*	96	–
	Carnivora	*Cerdocyon thous*	94	–
	Perissodactyla	*Tapirus terrestris*	41	–
	Artiodactyla	*Mazama gouazoubira*	55	G
	Rodentia	(P) *Akodon cursor*	255	S
	Rodentia	(G) *Akodon cursor*	23	S
	Primates	*Gorilla*	291	S, SP, SxSP
		Homo sapiens	267	S, G
		Pan	207	S, SP, SxSP
		Papio	364	S, SP, SxSP
		Alouatta	384	S, SP, SxSP
		Cebus	394	S, SP, SxSP
		Callithrix	505	S, SP
		Total	3,644	

In the last column are the sources of variation controlled for each taxon: S = sex; SP = species; SSP = subspecies; G = geography. Whenever one factor influenced differently each species or subspecies, the interactive effect was also controlled

Landmarks and Measurements

Three-dimensional coordinates were recorded for 34 landmarks (Fig. 1; Appendix Table 1) using a Microscribe 3DX (or MX, for smaller taxa) digitizer (Microscribe, IL) and some specimens with a Polhemus 3Draw digitizer (Colchester, VT). Details of the digitizing procedure are presented in Cheverud (1995). Landmarks are the same as in Marroig and Cheverud (2001), with the exception of the fronto-malare (FM). This landmark is located on the primate post-orbital bar, which is absent in other mammals. Landmarks were positioned at the intersection of sutures or other discrete (and homologous) cranial features, so that they could be easily identified in most mammal groups. This set of landmarks was chosen because it reflects important developmental and functional relationships among cranial structures while simultaneously representing the whole skull (Cheverud 1982; Marroig and Cheverud 2001). Nearly all landmarks were assumed to be homologous across the mammal groups sampled. Some taxa, however, exhibited only partial homology of two landmarks, because the temporal and/or frontal bones were expanded in such a way as to cover the sphenoidal area (*Akodon, Dasypus*). In these genera, the sutures formed by the parietal, frontal and alisphenoid bones (defining the PT landmark) and those formed by the temporal, alisphenoid and parietal bones (defining TSP) are replaced by a parieto-fronto-temporal suture (defined in these taxa as PT) and a temporo-alisphenoid-frontal suture (defined as TSP). PT is, therefore, placed distally in relation to TSP in these groups, the inverse position relative to all other taxa (Fig. 1a, Appendix).

A set of 35 linear measurements was then calculated from the landmark coordinates (Table 2). Bilaterally symmetrical measurements were averaged, and if the skull was damaged on one side, the other was used as the average. All specimens were measured twice, allowing the estimation of repeatability to account for measurement error (Falconer and Mackay 1996). Lilliefors tests were conducted for all measurements in order to check for significant deviations from normality. The average of repeated measurements was used in all subsequent analyses.

Correlation and Variance/Covariance Matrices

Sources of variation within each taxon that are not of immediate interest for this study (sex, geography, species, subspecies and their possible interactions) were explored through multivariate analysis of variance (MANOVA). Each source of variation in the model was tested using Wilk's lambda statistic and was considered significant when $P < 0.05$. Table 1 presents the sources of variation controlled for each taxon. Pooled within-group phenotypic correlation and variance/covariance matrices (hereafter referred to as correlation and V/CV matrices, for simplicity) were estimated for each taxon using the General Linear Model routine of SYSTAT 11 (SYSTAT Inc., Richmond, CA, 2004), controlling for these sources of variation whenever appropriate. The taxonomic arrangement and the variables controlled during the computation of Platyrrhini matrices (*Allouatta*, *Cebus*, *Callithrix*) are described elsewhere (Marroig and Cheverud 2001). With the exception of primates, taxa are referred to by their order name, for simplicity.

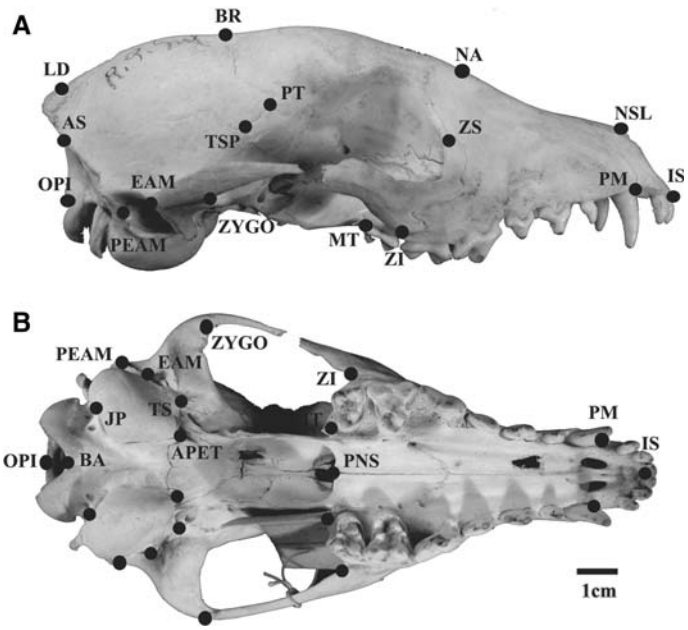

Fig. 1 Thirty four landmarks on the lateral (**a**) and ventral (**b**) view of a *Cerdocyon thous* cranium. Labels on (**b**) are placed only in one side of the skull. Landmark definitions are presented in Appendix. For exceptions regarding the position of landmarks, see text

Table 2 Cranial measurements and their association to the hypotheses of morphological integration formulated for each taxon studied

Measurement	Region	Hypotheses				
		Didelphimorphia, Dasyuromorphia, Peramelimorphia, Scandentia, Carnivora	Paucituberculata, Diprodontia, Hyracoidea, Macroscelidae	Cingulata, Lagomorpha, Rodentia	Perissodactyla, Artiodactyla	Primates
IS-PM	Face	Oral	Oral	Oral	Oral	Oral
IS-NSL	Face	Nasal	Nasal	Nasal	Nasal	Nasal
IS-PNS	Face	Oral, nasal	Oral, nasal	Oral, nasal	Oral, nasal	Oral, nasal
PM-ZS	Face	Oral	Oral	Oral	Oral	Oral
PM-ZI	Face	Oral	Oral	Oral	Oral	Oral
PM-MT	Face	Oral	Oral	Oral	Oral	Oral
NSL-NA	Face	Nasal	Nasal	Nasal	Nasal	Nasal
NSL-ZS	Face	Nasal	Nasal	Nasal	Nasal	Nasal
NSL-ZI	Face	Oral, nasal	Oral, nasal	Oral, nasal	Oral, nasal	Oral, nasal
NA-BR	Neurocranium	Vault	Vault	Vault	Vault	Vault
NA-PNS	Face	Nasal	Nasal	Nasal	Nasal	Nasal
BR-PT	Neurocranium	Vault	Vault	Vault	Vault	Vault
BR-APET	Neurocranium	Vault	Vault	Vault	Vault	Vault
PT-APET	Neurocranium	Vault	Vault	Vault	Vault	Vault
PT-BA	Neurocranium	Vault	Vault	Vault	Vault	Vault
PT-EAM	Neurocranium	Vault	Vault	Vault	Vault	Vault
PT-ZYGO	Face	Zygomatic	Zygomatic	Zygomatic	Zygomatic	Zygomatic
PT-TSP	Neurocranium, face	Vault, zygomatic	Vault, zygomatic	Vault, zygomatic	Vault, zygomatic	Vault, zygomatic
ZS-ZI	Face	Oral/zygo	Oral/zygo	Zygomatic	Oral	Oral
ZI-MT	Face	Oral	Zygomatic	Zygomatic	Oral	Oral
ZI-ZYGO	Face	Zygomatic	Zygomatic	Zygomatic	Zygomatic	Zygomatic
ZI-TSP	Face	Zygomatic	Zygomatic	Zygomatic	Zygomatic	Zygomatic
MT-PNS	Face	Oral	Oral	Oral	Oral	Oral
PNS-APET	Neurocranium	Base	Base	Base	Base	Base
APET-BA	Neurocranium	Base	Base	Base	Base	Base
APET-TS	Neurocranium	Base	Base	Base	Base	Base
BA-EAM	Neurocranium	Base	Base	Base	Base	Base
EAM-ZYGO	Face	Zygomatic	Zygomatic	Zygomatic	Zygomatic	Zygomatic
ZYGO-TSP	Face	Zygomatic	Zygomatic	Zygomatic	Zygomatic	Zygomatic
LD-AS	Neurocranium	Vault	Vault	Vault	Vault	Vault
BR-LD	Neurocranium	Vault	Vault	Vault	Vault	Vault
OPI-LD	Neurocranium	Vault	Vault	Vault	Vault	Vault
PT-AS	Neurocranium	Vault	Vault	Vault	Vault	Vault
JP-AS	Neurocranium	Vault	Vault	Vault	Vault	Base
BA-OPI	Neurocranium	Base	Base	Base	Base	Base

Genetic V/CV and correlation matrices were also produced for rodents (Rodentia G-matrix) using a dataset from a non-inbred colony of *Akodon cursor* (De Conto 2007). The breeding program was developed using 7 wild-caught males and 6 wild-caught females, and their descendants born in captivity (26 males and 27 females). The genealogies included grandparents, parents and their offspring, full-siblings, half-siblings and other relatives. Genetic (r_g) and environmental (r_e) correlations between characters were estimated by the maximum likelihood method using a multivariate animal model implemented in the SOLAR software package (Almasy and Blangero 1998). Genetic covariances were then estimated as the product of the appropriate correlation and associated standard deviations:

$$r_p \sigma_{px} \sigma_{py} = r_g h_x \sigma_{px} h_y \sigma_{py} + r_e e_x \sigma_{px} e_y \sigma_{py}$$

where r_p is the phenotypic correlation between traits x and y, σ_{px} is the phenotypic standard deviation for trait x, σ_{py} is the phenotypic standard deviation for trait y, r_g is the genetic correlation between traits x and y, h_x is the square root of heritability for trait x, h_y is the square root of heritability for trait y, r_e is the environmental correlation between traits x and y, e_x is the square root of one minus heritability for trait x, and e_y is the square root of one minus heritability for trait y (Falconer and Mackay 1996).

Matrix Comparisons and Matrix Repeatability

Covariance patterns were compared among mammalian orders using the random skewers method, in which the evolutionary responses of each pair of V/CV matrices to 1,000 random selection vectors (normalized to a length of one) are compared (Cheverud and Marroig 2007). The comparison is done computing the vector correlation between the responses of the two matrices to each random selection vector. The vector correlation is given by the cosine of the angle between any two vectors. The average vector correlation between the matrix response vectors was used as the measure of similarity. The expected range of correlations commonly occurring among 35-element vectors by chance alone is $-0.45 < r < 0.45$, but only absolute values need to be taken into consideration because an angle of $\theta > 90°$ is equivalent to one of $180° - \theta$. To establish the significance of the vector correlation we used a broken stick model to obtain 1,000 random 35-element vectors from a uniform distribution to correlate each random vector to any fixed random vector (we used a fixed isometric vector with elements equal to 0.169). Our sample showed an average correlation of 0.143 and a SD = 0.107, both values being nearly the same, no matter which fixed vector was compared to the random vectors. These two statistics, based on a random sample of 35-element vectors, allow us to test whether or not the correlation of any two observed vectors is significantly different from the correlation between two vectors expected by chance. Accordingly, any vector correlation larger than 0.45 were deemed significant at $P < 0.001$ (see Marroig and Cheverud 2005; Cheverud and Marroig 2007 for more details).

Correlation matrices were compared using matrix correlation (Sneath and Sokal 1973), and statistical significance was evaluated using Mantel's test. This procedure compares the original matrix correlation with a distribution of matrix correlations expected by chance alone. This random distribution was derived from a comparison between one of the compared matrices and 10,000 permuted versions of the second matrix, obtained through random permutations of columns and associated rows. If the original correlation exceeded 95% of these randomly simulated correlations, the matrices were considered significantly similar (Cheverud et al. 1989).

Sample size can affect the estimation of individual matrix elements due to sampling error. Thus, when evaluating structural similarity between correlation matrices, one must take into account that the maximum observable correlation between two matrices is not one. Instead, it is equal to a maximum correlation, r_{max}, defined as:

$$r_{max} = (t_1 \times t_2)^{1/2},$$

where t_1 and t_2 are the repeatabilities of matrices 1 and 2, respectively (Cheverud 1996). Accordingly, matrix correlation can be rewritten as a proportion of r_{max} as follows:

$$r_{adj} = r_{obs}/r_{max},$$

where r_{obs} is the observed matrix correlation and r_{adj} is the adjusted matrix correlation.

Correlation matrix repeatabilities were estimated following Cheverud (1996). V/CV matrix repeatabilities were calculated using a Monte Carlo approach, in which one hundred bootstrap re-samplings of the original data were made (after removing other sources of variation, as described above and in Table 1), with the sample size held constant. V/CV matrices were calculated for each of the re-samples and compared to the original matrix using the random skewers method (outlined above). The average vector correlation was then used as a measure of the repeatability (t). Observed vector correlations were adjusted for repeatabilities as described above for correlation matrices.

The effective sample size was used as the size of the population sample to estimate Rodentia G-matrix repeatability. The effective sample size is the effective number of paired breeding values represented in the genealogical data and used in estimating any given genetic correlation. It is calculated as:

$$N_{eff} = \left\{ 2h_x^2 2h_y^2 / \left[V\left(h_x^2\right) V\left(h_y^2\right) \right]^{1/2} \right\} + 1,$$

where $V(h^2)$ is the variance of the heritability (square of the standard error) (Cheverud 1995, 1996).

Morphological Integration Hypotheses

In order to test hypotheses of morphological integration in the mammalian skull, matrix correlations were calculated between the observed correlation matrices and theoretical matrices based on functional/developmental relationships among characters (Table 2), following Cheverud (1995, 1996) and Marroig and Cheverud (2001). These matrices were constructed to test for significant integration in the

two major regions of the skull, neurocranium and face, as well as five sub-regions: oral, zygomatic, nasal, cranial base and cranial vault. The theoretical matrices were constructed as follows: whenever two traits belonged to the same functional/developmental set being tested (i.e., hypothesized module), a value of one was entered in the matrix; otherwise, a value of zero was entered. Additionally, two more matrices were constructed: the first one links all neural and, separately, all facial traits, testing for neural (early) versus somatic (later) growth integration; and the second combines all five cranial sub-regions in a single matrix, testing for 'total' integration. Whenever a cell in this matrix had a value greater than one, it was reduced to one. Mantel's tests were used to assess statistically significant similarities between the taxa correlation matrices and each theoretical matrix. For more details of this procedure and its theoretical background, refer to Cheverud (1995, 1996).

Pearson's correlation coefficient averages for integrated (avg+) and non-integrated (avg−) traits were calculated for each integration hypothesis. The ratio between the average of integrated and non-integrated traits provides information on the magnitude of integration within the proposed phenotypic modules in relation to all remaining traits. This ratio can also be envisaged as a measure of modular distinctiveness within each taxon. If correlations within a module are, on average, higher than correlations in other modules (or between modules) the ratio will be larger than one; if not, the ratio will be smaller than one.

Magnitude of Integration

The overall magnitude of integration within each matrix was evaluated through the calculation of the coefficient of determination (r^2) of the correlation matrices (see Cheverud et al. 1989). This coefficient is simply the average of squared correlation coefficients and measures the overall level of integration among all traits. The r^2 is also a scale-independent index and is particularly suitable to compare taxa with very different sizes, such as the mammal groups studied here. It should be noted, however, that r^2 refers to a general property of the correlation matrices (*overall level of integration*) and has no direct connection to the level of integration within and between phenotypic modules (*modular level of integration*), as explored by the tests of morphological integration hypotheses. In order to compare differences in the magnitude of integration with similarity in patterns of integration we also calculated a dissimilarity matrix based on the r^2 values determined for each matrix. This matrix is calculated simply by square-rooting the differences in r^2 for each pair of matrices compared.

Phylogeny and Modularity Patterns

The phylogenetic hypothesis adopted throughout this study (Fig. 2) follows the pattern recovered by most recent analyses (Murphy et al. 2001; Springer et al. 2004; Beck et al. 2006; Asher 2007). The topology seems to be well resolved and supported by many genes and character

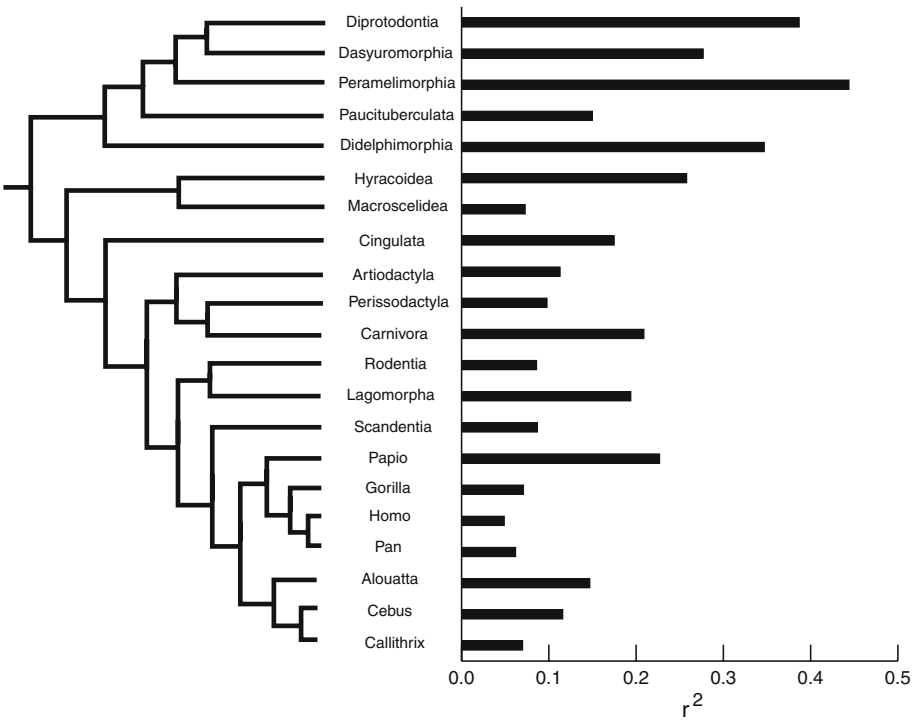

Fig. 2 The phylogenetic hypothesis adopted in this study (see text for references) associated to the overall morphological integration index (r^2) for each terminal

combinations (Beck et al. 2006). In order to test the association of the phylogeny with the similarity in correlation/covariance patterns, a phylogenetic distance matrix was constructed from the branch length data provided by Beck et al. 2006. This matrix was then compared, via matrix correlation followed by Mantel's test, to the similarity matrix derived from the comparison of correlation and V/CV matrices among all taxa as well as to the r^2 dissimilarity matrix.

Results

Measurement Error Assessment

The repeatability of the dataset calculated separately for each of the 35 characters and taxon ranged from 0.86 to 1.00 (mean = 0.97, s.d. = 0.03). In general, all traits were normally distributed within groups. The number of measurements with significant deviation from a normal distribution (average of one per taxon) is within the range expected by chance alone on multiple tests (considering $\alpha = 0.05$). No taxon had more than four measurements with non-normal distribution and, therefore, no impact from these sources is expected in subsequent analyses.

Correlation and Covariance Structure

Raw and adjusted matrix correlations between mammal correlation matrices, along with the respective matrix repeatabilities, are presented in Table 3. In general, there was considerable similarity in the correlation and covariance structure of all matrices compared. With the exception of the comparison between Perissodactyla and Rodentia G-matrix ($P = 0.052$), all raw matrix correlations were significant at the 0.05 level, and 96% of them were also significant at the 0.001 level. Raw correlations ranged from 0.12 to 0.83 (mean = 0.45) and adjusted correlations ranged from 0.22 to 1.05 (mean = 0.58). Lower correlation values ($r < 0.3$) were associated with comparisons involving *Homo*, *Gorilla* and the Rodentia G-matrix. Higher levels ($r > 0.6$) were observed in comparisons between metatherian taxa, hyracoids, lagomorphs and carnivores, as well as within primates. Adjustment for matrix repeatability did not change the general pattern of similarity, but comparisons involving macroscelids, cingulates, scandents, perissodactyls and artiodactyls appeared among the highest correlations only when adjusted, due to their lower matrix repeatabilities. A noteworthy increase in similarity levels when accounting for repeatability was also observed when comparing the genera *Papio* and *Alouatta* with the metatherian orders and hyracoids: in these cases, the adjusted values reached levels comparable to those found within primate genera.

Raw and adjusted vector correlations between V/CV matrices are in Table 4. Raw vector correlations varied from 0.41 to 0.88 (mean = 0.66), and adjusted vector correlations ranged from 0.42 to 0.99 (mean = 0.70). The similarity pattern observed for V/CV matrices among taxa was generally the same as observed for the correlation matrices (matrix correlation of 0.731, $P = 0.0002$); it should be noted that higher levels of similarity were found when comparing V/CV matrices (47% higher, on average).

Comparisons involving the only genetic matrix in our dataset, Rodentia G-matrix, were no exception to the overall pattern of similarity found among the taxa studied. When adjusted to matrix repeatability, a high degree of shared correlation/covariance structure was observed. When comparing correlation matrices with Rodentia G-matrix, adjusted values ranged from 0.22 to 1.08 (mean = 0.47), and the corresponding V/CV matrix similarities were even higher (ranged from 0.67 to 0.99; mean = 0.73). In some instances, comparing the Rodentia G-matrix with distantly related taxa, like metatherians, yielded higher similarities than those found when comparing phylogenetically close groups, like two primate genera.

Magnitude of Integration

Higher r^2 values, indicating higher overall level of integration, were mainly associated with metatherian taxa, with the highest value observed for peramelimorphs ($r^2 = 0.44$; Fig. 2). Other highly integrated taxa were hyracoids, lagomorphs, carnivores, cingulates and *Papio*. Even including the latter exceptions, the average r^2 value for eutherians is three times lower than for metatherians (0.13 and 0.32, respectively). Lower r^2 values included rodents, scandents, macroscelids, and most of the primates. The lowest value was found in *Homo* ($r^2 = 0.048$).

Morphological Integration

The Mantel association tests of the theoretical hypotheses of morphological integration and observed correlation matrices are presented in Table 5, with boldface values for correlations significant at $P < 0.05$ and italics for $P < 0.10$. In general, matrix correlations between total integration and observed matrices were all positive and significant for eutherian taxa ($P < 0.05$), except for lagomorphs and hyracoids. Comparisons involving macroscelids and carnivores yielded marginally significant probability values ($0.05 < P < 0.10$). None of the metatherian taxa matrices were significantly correlated with the total integration matrix.

Table 3 Similarity matrix among mammalian taxa correlation matrices for raw (below diagonal) and adjusted (above diagonal) correlations

		1	2	3	4	5	6	7	8	9	10	11	12	13	14	15	16	17	18	19	20	21	22
1.	Didelphimorphia	**0.92**	0.81	0.73	0.77	0.63	0.69	0.52	0.50	0.67	0.74	0.80	0.69	0.60	0.51	0.38	0.39	0.35	0.54	0.53	0.78	0.59	0.42
2.	Paucituberculata	0.68	**0.77**	0.80	0.81	0.76	0.85	0.71	0.56	0.85	0.78	0.86	0.65	0.61	0.66	0.61	0.30	0.32	0.63	0.68	0.73	0.64	0.47
3.	Dasyuromorphia	0.62	0.62	**0.79**	0.97	1.05	0.81	0.66	0.49	0.73	0.86	0.71	0.50	0.47	0.58	0.50	0.25	0.36	0.54	0.66	0.69	0.52	0.39
4.	Diprotodontia	0.68	0.66	0.80	**0.85**	0.90	0.97	0.60	0.54	0.63	0.90	0.74	0.49	0.53	0.59	0.46	0.29	0.31	0.59	0.70	0.74	0.63	0.40
5.	Peramelimorphia	0.54	0.59	0.83	0.74	**0.79**	0.73	0.53	0.42	0.63	0.83	0.67	0.44	0.32	0.55	0.39	0.25	0.22	0.56	0.75	0.64	0.44	0.29
6.	Hyracoidea	0.58	0.66	0.64	0.80	0.58	**0.79**	0.69	0.46	0.72	0.86	0.67	0.41	0.61	0.53	0.40	0.25	0.28	0.55	0.58	0.74	0.65	0.44
7.	Macroscelidea	0.40	0.49	0.46	0.44	0.37	0.48	**0.62**	0.75	0.79	0.58	0.66	0.66	0.75	0.72	0.56	0.33	0.53	0.64	0.50	0.61	0.60	0.72
8.	Cingulata	0.41	0.43	0.38	0.43	0.32	0.36	0.52	**0.76**	0.59	0.54	0.66	0.71	0.77	0.65	0.50	0.45	0.44	0.54	0.54	0.47	0.37	0.57
9.	Scandentia	0.50	0.59	0.50	0.45	0.43	0.50	0.49	0.40	**0.61**	0.61	0.74	0.49	0.67	0.66	0.54	0.29	0.37	0.48	0.45	0.63	0.66	0.67
10.	Lagomorpha	0.65	0.63	0.70	0.76	0.67	0.70	0.42	0.43	0.44	**0.84**	0.74	0.66	0.61	0.64	0.53	0.29	0.32	0.60	0.58	0.69	0.52	0.39
11	Carnivora	0.65	0.64	0.54	0.58	0.51	0.51	0.45	0.49	0.49	0.57	**0.73**	0.84	0.76	0.53	0.50	0.54	0.51	0.71	0.63	0.71	0.68	0.57
12.	Perissodactyla	0.48	0.41	0.32	0.32	0.28	0.26	0.37	0.45	0.28	0.43	0.52	**0.52**	0.66	0.50	0.26	0.50	0.46	0.62	0.40	0.57	0.41	0.45
13.	Artiodactyla	0.48	0.44	0.35	0.41	0.23	0.45	0.49	0.56	0.44	0.46	0.54	0.40	**0.69**	0.49	0.26	0.47	0.45	0.56	0.46	0.56	0.53	0.59
14.	Rodentia (P)	0.46	0.54	0.49	0.52	0.46	0.44	0.54	0.54	0.49	0.56	0.43	0.34	0.39	**0.90**	1.08	0.28	0.49	0.57	0.56	0.59	0.52	0.52
15.	Rodentia (G)	0.24	0.35	0.29	0.28	0.23	0.23	0.29	0.29	0.28	0.32	0.28	0.12	0.14	0.67	**0.43**	0.22	0.41	0.52	0.50	0.48	0.46	0.45
16.	*Gorilla*	0.35	0.25	0.21	0.25	0.21	0.20	0.24	0.37	0.21	0.25	0.43	0.34	0.37	0.25	0.13	**0.87**	0.61	0.68	0.47	0.53	0.50	0.43
17.	*Homo*	0.31	0.26	0.30	0.27	0.18	0.23	0.38	0.35	0.27	0.27	0.40	0.31	0.35	0.43	0.25	0.53	**0.85**	0.63	0.32	0.51	0.55	0.55
18.	*Pan*	0.47	0.51	0.44	0.50	0.45	0.45	0.47	0.43	0.34	0.50	0.56	0.41	0.43	0.50	0.31	0.58	0.53	**0.84**	0.70	0.72	0.68	0.57
19.	*Papio*	0.50	0.58	0.57	0.63	0.65	0.50	0.39	0.46	0.34	0.52	0.53	0.28	0.37	0.52	0.32	0.43	0.28	0.63	**0.95**	0.67	0.50	0.40
20.	*Alouatta*	0.73	0.62	0.59	0.66	0.55	0.63	0.47	0.40	0.47	0.61	0.59	0.40	0.45	0.54	0.31	0.48	0.45	0.65	0.63	**0.94**	0.81	0.66
21.	*Cebus*	0.55	0.54	0.45	0.56	0.38	0.56	0.46	0.31	0.50	0.46	0.57	0.29	0.43	0.48	0.29	0.45	0.49	0.61	0.47	0.76	**0.95**	0.72
22.	*Callithrix*	0.39	0.40	0.33	0.36	0.25	0.37	0.55	0.47	0.50	0.34	0.47	0.31	0.48	0.47	0.28	0.39	0.49	0.51	0.38	0.62	0.67	**0.93**

Matrix repeatabilities are on the diagonal, in boldface. Almost all correlations are significant at $P < 0.05$. Non significant values ($P > 0.05$) are underlined

Table 4 Similarity matrix among mammalian taxa V/CV matrices for raw (below diagonal) and adjusted (above diagonal) correlations

		1	2	3	4	5	6	7	8	9	10	11	12	13	14	15	16	17	18	19	20	21	22
1.	Didelphimorphia	**0.93**	0.82	0.92	0.89	0.88	0.82	0.67	0.78	0.76	0.85	0.92	0.77	0.76	0.75	0.79	0.59	0.57	0.64	0.79	0.79	0.62	0.59
2.	Paucituberculata	0.77	**0.96**	0.76	0.82	0.82	0.75	0.73	0.78	0.72	0.80	0.78	0.70	0.76	0.78	0.70	0.43	0.42	0.56	0.76	0.63	0.47	0.48
3.	Dasyuromorphia	0.87	0.73	**0.96**	0.87	0.86	0.80	0.66	0.72	0.74	0.81	0.88	0.70	0.71	0.70	0.74	0.56	0.55	0.65	0.76	0.79	0.61	0.57
4.	Diprotodontia	0.84	0.79	0.84	**0.97**	0.89	0.86	0.69	0.80	0.72	0.86	0.85	0.70	0.78	0.76	0.75	0.52	0.49	0.61	0.79	0.73	0.57	0.56
5.	Peramelimorphia	0.84	0.80	0.83	0.87	**0.98**	0.82	0.66	0.80	0.71	0.83	0.84	0.69	0.74	0.73	0.72	0.50	0.44	0.57	0.80	0.67	0.48	0.49
6.	Hyracoidea	0.78	0.72	0.76	0.83	0.80	**0.96**	0.73	0.80	0.70	0.83	0.80	0.68	0.78	0.74	0.69	0.48	0.49	0.58	0.71	0.73	0.59	0.58
7.	Macroscelidea	0.63	0.68	0.62	0.65	0.63	0.69	**0.93**	0.75	0.71	0.73	0.69	0.69	0.81	0.81	0.69	0.50	0.55	0.67	0.66	0.67	0.55	0.65
8.	Cingulata	0.75	0.75	0.69	0.78	0.78	0.77	0.71	**0.98**	0.67	0.81	0.76	0.67	0.84	0.75	0.68	0.46	0.41	0.56	0.76	0.60	0.43	0.49
9.	Scandentia	0.71	0.68	0.70	0.69	0.68	0.67	0.66	0.64	**0.95**	0.75	0.80	0.71	0.76	0.81	0.77	0.56	0.58	0.64	0.60	0.70	0.73	0.75
10.	Lagomorpha	0.81	0.78	0.78	0.84	0.81	0.80	0.69	0.79	0.72	**0.97**	0.86	0.75	0.83	0.83	0.76	0.52	0.51	0.63	0.74	0.72	0.54	0.56
11.	Carnivora	0.88	0.76	0.85	0.83	0.82	0.77	0.66	0.74	0.77	0.83	**0.97**	0.76	0.80	0.77	0.79	0.59	0.59	0.68	0.77	0.81	0.67	0.65
12.	Perissodactyla	0.71	0.65	0.66	0.66	0.65	0.64	0.64	0.64	0.66	0.71	0.72	**0.92**	0.77	0.71	0.67	0.66	0.63	0.71	0.68	0.68	0.57	0.62
13.	Artiodactyla	0.72	0.73	0.68	0.75	0.71	0.75	0.75	0.81	0.72	0.80	0.77	0.71	**0.95**	0.79	0.68	0.54	0.51	0.65	0.70	0.68	0.55	0.62
14.	Rodentia (P)	0.70	0.74	0.66	0.72	0.69	0.69	0.75	0.72	0.75	0.79	0.73	0.66	0.74	**0.93**	0.99	0.60	0.65	0.71	0.71	0.72	0.64	0.70
15.	Rodentia (G)	0.64	0.58	0.61	0.63	0.60	0.57	0.56	0.57	0.63	0.64	0.66	0.54	0.56	0.81	**0.72**	0.68	0.70	0.73	0.70	0.75	0.71	0.74
16.	*Gorilla*	0.57	0.41	0.55	0.51	0.49	0.46	0.48	0.45	0.54	0.51	0.58	0.63	0.52	0.57	0.57	**0.98**	0.84	0.74	0.54	0.62	0.63	0.71
17.	*Homo*	0.55	0.41	0.53	0.48	0.43	0.47	0.52	0.40	0.56	0.50	0.58	0.60	0.49	0.62	0.59	0.82	**0.98**	0.75	0.48	0.70	0.72	0.77
18.	*Pan*	0.61	0.54	0.62	0.60	0.55	0.56	0.63	0.54	0.61	0.61	0.67	0.67	0.62	0.67	0.61	0.72	0.73	**0.97**	0.71	0.78	0.67	0.70
19.	*Papio*	0.76	0.74	0.74	0.77	0.79	0.69	0.63	0.75	0.58	0.73	0.76	0.65	0.68	0.68	0.59	0.54	0.47	0.70	**0.99**	0.69	0.48	0.49
20.	*Alouatta*	0.76	0.62	0.77	0.72	0.66	0.71	0.64	0.59	0.68	0.70	0.80	0.65	0.66	0.69	0.63	0.61	0.69	0.77	0.68	**0.99**	0.81	0.75
21.	*Cebus*	0.60	0.46	0.59	0.56	0.48	0.58	0.53	0.43	0.70	0.53	0.66	0.55	0.53	0.62	0.59	0.63	0.71	0.66	0.48	0.80	**0.99**	0.86
22.	*Callithrix*	0.56	0.47	0.56	0.54	0.48	0.57	0.62	0.48	0.72	0.55	0.63	0.59	0.60	0.67	0.62	0.70	0.76	0.69	0.49	0.74	0.85	**0.99**

Matrix repeatabilities are on the diagonal, in boldface. All correlations are significant at $P < 0.05$

Table 5 Ratio between the magnitude of integrated (avg+) and non-integrated (avg−) traits for each theoretical hypothesis

Group	Oral	Nasal	Zygo	Vault	Base	Face	Neurocranium	Neuroface	Total
Didelphimorphia	*1.20*	*1.26*	1.18	0.90	0.73	*1.18*	0.82	1.01	1.04
Paucituberculata	**1.97**	**2.03**	1.12	0.56	0.48	**1.85**	0.48	**1.15**	1.08
Dasyuromorphia	1.25	1.35	1.21	0.79	0.52	**1.35**	0.70	1.04	0.99
Diprotodontia	**1.43**	**1.47**	1.04	0.74	0.72	**1.34**	0.67	1.01	1.00
Peramelimorphia	**1.32**	*1.26*	1.03	0.80	0.78	**1.24**	0.79	1.03	1.00
Hyracoidea	**1.71**	**1.75**	1.32	0.68	0.40	**1.67**	0.55	**1.11**	1.10
Macroscelidea	**2.63**	**2.02**	0.64	0.87	0.01	**1.74**	0.66	**1.27**	*1.24*
Cingulata	**1.70**	**1.66**	0.60	1.16	0.52	1.09	0.98	1.06	**1.15**
Scandentia	**1.68**	*1.60*	0.93	1.18	0.48	*1.33*	1.01	**1.29**	**1.31**
Lagomorpha	**1.75**	**1.75**	0.82	0.79	0.51	**1.33**	0.71	1.03	1.02
Carnivora	**1.34**	**1.52**	0.98	0.87	0.90	**1.22**	0.83	*1.05*	*1.08*
Perissodactyla	**2.09**	**1.86**	0.70	1.01	0.63	*1.32*	0.84	*1.13*	**1.38**
Artiodactyla	**1.97**	1.36	0.55	1.28	0.09	1.13	0.96	1.08	**1.35**
Rodentia (P)	**1.72**	**2.32**	0.94	1.11	0.70	**1.41**	0.94	**1.29**	**1.33**
Rodentia (G)	1.04	**1.90**	1.28	1.18	0.65	**1.35**	0.99	**1.30**	**1.27**
Gorilla	**1.67**	1.12	1.21	**1.37**	0.62	*1.24*	1.00	**1.20**	**1.40**
Homo	**1.80**	1.27	1.34	**1.87**	0.98	1.06	**1.38**	**1.35**	**1.85**
Pan	**2.55**	**2.07**	1.41	0.80	0.63	**1.93**	0.63	**1.37**	**1.57**
Papio	**1.68**	**1.62**	1.22	0.67	0.70	**1.68**	0.62	**1.19**	**1.12**
Allouatta	**1.82**	1.33	1.21	0.93	0.61	**1.47**	0.76	**1.17**	**1.24**
Cebus	**2.05**	1.39	1.35	0.98	0.98	**1.55**	0.80	**1.27**	**1.44**
Callithrix	**2.20**	1.43	0.98	1.19	0.72	1.18	0.99	*1.15*	**1.50**

Values in bold indicate the positive and significant correlations at $P < 0.05$ and in italics for marginally significant ($P < 0.1$) for the Mantel tests of morphological integration. The "zygomatic" and "cranial base" results are not shown because there was no association with any of the mammal taxa matrices (see text)

Matrix correlations between the neuro-somatic matrix and most of the eutherian taxa were also positive and significant, except for lagomorphs, artiodactyls and cingulates; carnivores and perissodactyls were marginally significant. The only metatherian with significant neuro-somatic integration was Paucituberculata. The neural integration matrix, in contrast, was significantly correlated with only one taxon in the whole sample, *Homo* ($P = 0.05$). The facial region presented positive and significant integration for almost all taxa, with the exception of cingulates, artiodactyls, humans and marmosets. It is noteworthy that all other primates presented highly significant correlations with the facial region matrix.

Among the five cranial sub-regions, only vault, nasal and oral exhibited positive and significant correlation with the mammal taxa matrices; therefore, we report only results referring to these three sub-regions (Table 5). The vault matrix was positively and significantly correlated only with *Homo* and *Gorilla* matrices. The oral matrix, in contrast, was correlated with almost all groups, except for Rodentia G-matrix and Dasyuromorphia. The nasal matrix exhibited positive and significant correlations for most groups, with the exception of dasyuromorphs, artiodactyls and the primates *Gorilla*, *Homo*, *Allouatta*, *Cebus* and *Callithrix*.

Table 5 also reports, for each morphological integration hypothesis, the ratio (avg+/avg−) between the average of correlation coefficients for the integrated (avg+) and non-integrated traits (avg−). One point particularly important to be noted is the negative association of these ratios with the morphological integration index (r^2 values) of each taxon: taxa presenting higher ratio (avg+/avg−) tended to present lower r^2 values, and vice versa. This can be readily seen in the plots of the avg+/avg− ratios for five of the theoretical hypotheses against the morphological integration index (r^2) (Fig. 3).

Comparisons of Patterns and Levels of Integration with Phylogenetic Distances

Figure 2 presents the phylogenetic hypothesis used in this study associated with the respective coefficients of determination of the correlation matrices (r^2), which is an index of the overall level of integration. Measures of correlation and V/CV pattern similarity did not correlate significantly with phylogenetic distance (V/CV: $r = -0.048$; $P = 0.271$; correlation: $r = -0.068$; $P = 0.237$). However, the magnitude of the differences in the overall magnitude of correlation coefficients (i.e., pairwise differences in r^2

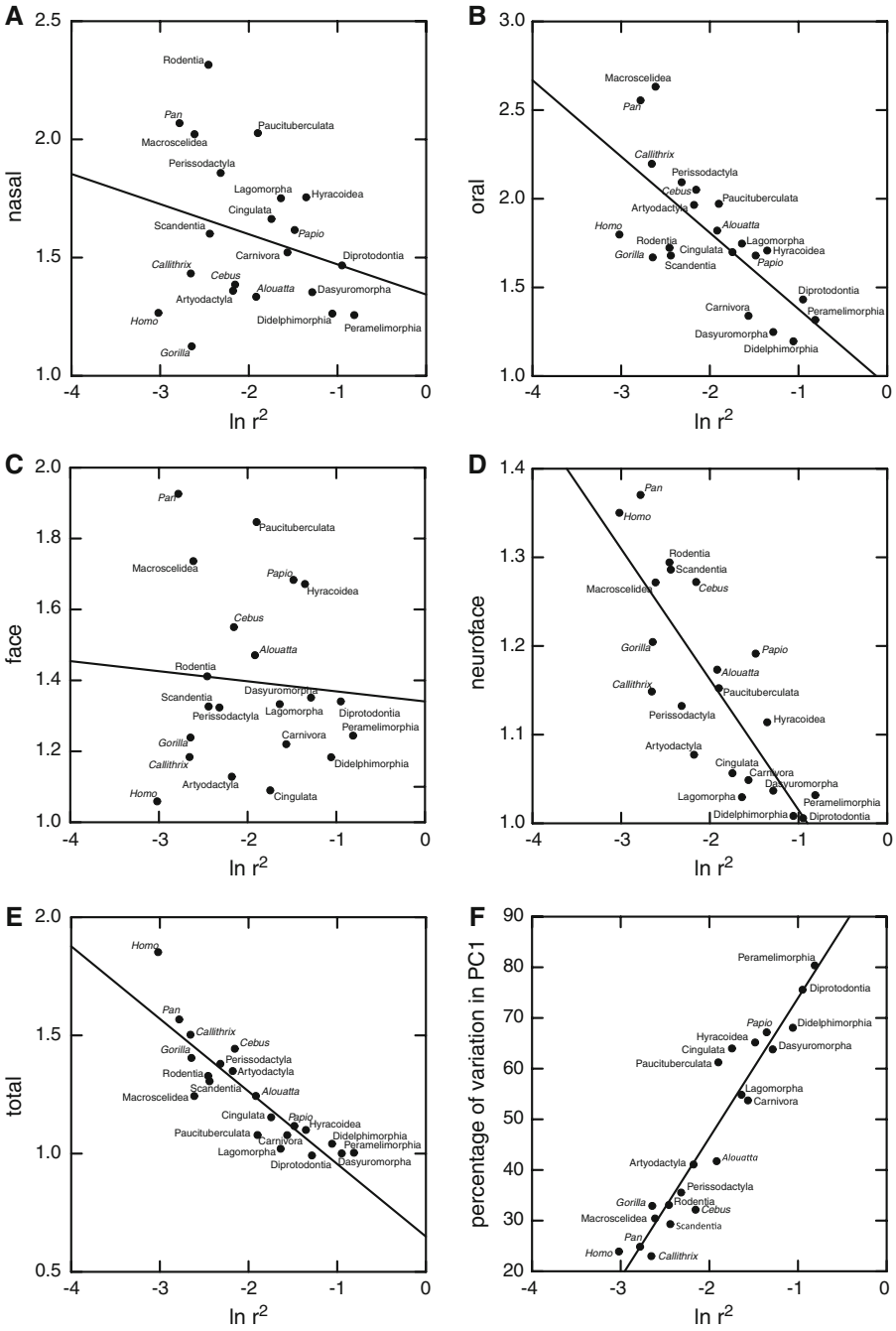

Fig. 3 Scatterplots of the relationships between the overall morphological integration index (r^2) and the ratio of integrated and non-integrated traits (avg+/avg−) for five of the theoretical modularity hypothesis investigated: nasal (**a**), oral (**b**), face (**c**), neuroface (**d**), and total (**e**). (**f**) Shows the relationship between r^2 and the percentage of variation explained by the first principal component of each taxon matrix, which is an indication of the amount of variation attributable to size. r^2 was log-transformed to linearize relationships

between taxa) were significantly associated with the phylogenetic distances ($r = 0.491$; $P < 0.001$).

Discussion

Correlation and Variance/Covariance Structure

In this study, levels and patterns of morphological integration in the skull were compared among several mammal groups. Direct comparisons of both correlation and V/CV matrices revealed a moderate to high level of similarity between all groups investigated. With the exception of *Homo* and *Gorilla*, which exhibited fairly lower values than other groups, the observed level of similarity was homogeneously distributed across all comparisons. This suggests that the overall integration pattern of cranial morphological elements has remained unexpectedly similar during mammalian morphological diversification.

V/CV matrix comparisons yielded higher similarities (47% higher, on average) than comparisons between correlation matrices, a common result in similar analyses (e.g.,

Marroig and Cheverud 2001). When matrix repeatability was accounted for, such difference was reduced by half. Considering that matrix repeatability is strongly influenced by sampling error, these differences are probably related to the higher sensitivity of correlation matrix comparison methods to outliers and sampling error. The random skewers method, used here to compare V/CV matrices, was demonstrated to be less sensitive to small sample sizes than other matrix comparison methods (Cheverud and Marroig 2007); therefore, it is reasonable to hypothesize that element-wise matrix correlation, the method used in this study to compare correlation matrices, is relatively more sensitive to small sample sizes. Another possibility is that the distribution of correlations within the correlation matrices are non-normal, rendering parametric methods inadequate to this kind of data (Cheverud et al. 1989).

Nevertheless, the pattern of overall similarity holds for both correlation and covariance matrix comparisons. Especially noteworthy are the high similarities detected between the phenotypic covariance structure in the skull of all sampled mammals and the Rodentia G-matrix. The relationship between phenotypic and genetic V/CV matrices has been a disputed topic for long (e.g., Cheverud 1988; Willis et al. 1991; Roff 1997; Steppan et al. 2002), particularly because the evolutionary constancy (or proportionality) of the G-matrix, as well as the similarity with its phenotypic counterpart, are important premises for the application of Quantitative Genetics models to the study of macroevolution (Lande 1979; Steppan et al. 2002). In this context, our findings lead to the provocative suggestion that not only P-matrices are similar to G-matrices, but also that both remained remarkably stable for a long evolutionary period, despite extensive morphological change and environmental shifts. One alternative explanation would be that the corresponding environmental matrices changed in such a way to mask eventual evolutionary modifications on the G-matrix, which is highly improbable considering the number of taxa analyzed and the time scale involved. The similarity between P and G-matrices was already demonstrated, at least for morphological traits, for a variety of taxa, including several mammals groups (Cheverud 1988; Roff 1997; Ackermann and Cheverud 2000; Marroig and Cheverud 2001). Yet, it is important to keep in mind that G- and P-matrices compared here are not strictly constant or equal. In fact, it is highly improbable that any mammalian population would have strictly the same covariance structure (pattern and magnitude) that any other population. This is a simple corollary of the fact that any population is a unique entity formed by a number of individuals that carry part of the total genetic diversity of the species at all loci (with their multitude of interactions). Therefore, it is expected a priori that any population with sexual reproduction and recombination would have a distinct variance/covariance matrix. In this context, the question we try to address here is: how similar the skull V/CV structure is across mammals? The answer is that in most situations they are sufficiently similar to allow comparative quantitative genetics studies to be performed on P-matrices with reasonable confidence (Marroig and Cheverud 2001; Marroig et al. 2008).

The remarkable similarity in correlation/covariance patterns described here is in agreement with previous observations of common developmental patterns in the skull of mammals (Moore 1981; Smith 1997), and even in tetrapods as a whole (Morriss-Kay 2001; Helms et al. 2005; Tapadia et al. 2005). Such agreement might be evidence that the conserved pattern of inter-trait relationships is maintained by internal stabilizing selection (Cheverud 1996; Marroig and Cheverud 2001). This pattern results from the requirement of structural cohesion within an organism, so that the development and function of the cranium are preserved along the diversification of lineages. Since this cohesion imposes certain limitations to individual variation, its preservation within and among populations constrains the variation available to external selection in these groups, through its effects over the genetic correlations (Cheverud 1984). Additionally, while external selection (or even drift) could theoretically cause departures from this pattern of variation, our results suggest that such deviations were small, often restricted to a specific functional sub-region of the skull (see *Modularity*). Despite the overall pattern of similarity, it should be noted that covariance structure was not strictly equal in any of the comparisons, and these differences in V/CV and correlation matrices were not significantly associated with phylogenetic history. In some instances, like in the primate genus *Papio*, the correlation/covariance structure was more similar to those of distantly related taxa, like metatherians, than to other primates (Tables 3 and 4). Therefore, in the taxa investigated here, the evolution of correlation/covariance structure seems to be relatively independent of phylogenetic history. Such dissociation has already been observed for other taxa (Marroig and Cheverud 2001; Begin and Roff 2005; Roff and Mousseau 2005; Revell et al. 2007). Moreover, our data suggest that the same basic relationships between traits might produce great variation in skull morphology, as seen in New World monkeys (Cheverud 1996; Ackermann and Cheverud 2000; Marroig and Cheverud 2001). The level of similarity reported here can be considered quite high, especially because these comparisons involve two large and inclusive sister groups, Metatheria and Eutheria, that diverged at least 65 million years ago (MYA) and perhaps as far back as 147 MYA (Beck et al. 2006; Wible et al. 2007; Kitazoe et al. 2007). This finding indicates that the pattern of inter-trait

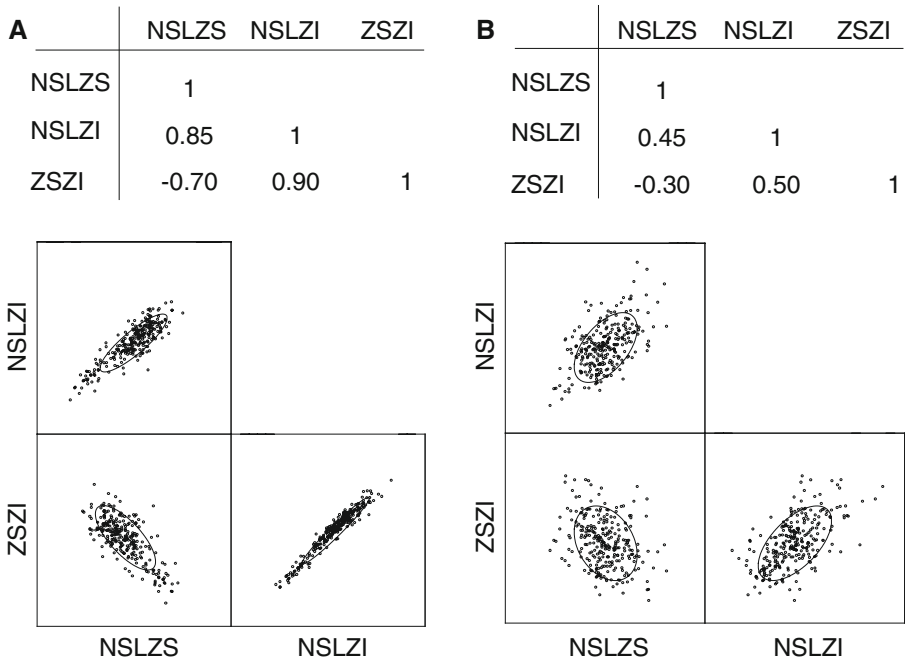

Fig. 4 Table of correlations between three skull measurements of two hypothetical species, A and B, and their respective scatterplots. In this situation, species have exactly the same pattern of inter-trait relationships, but differ in the magnitude of the correlations (species A presents higher magnitude of integration than B; note that traits are more tightly associated in A than in B). The example is hypothetical, but a very similar situation is seen when comparing *Didelphis* and *Homo*, for instance

relationships has remained strikingly similar during an extensive time period, and underlies the diversity existent in the skull of all mammalian groups investigated here. This apparently paradoxical result can only be interpreted when considered conjointly with the results on the magnitude of integration.

While the correlation/covariance patterns remained similar, the overall magnitude of integration (r^2) exhibited substantial differentiation among groups. More derived eutherians, in general, had lower r^2 values when compared to metatherians and more basal eutherian taxa (e.g., hyracoids and cingulates), being particularly low among most primates. The values of r^2 for methaterians were almost four times higher than those of most monkeys (Fig. 2), suggesting a more constrained cranium, in evolutionary terms, among metatherians (see companion paper: Marroig et al. 2008). There were, however, exceptions to this trend (i.e., eutherians with relatively high r^2 values), like Lagomorpha, Carnivora, and especially *Papio*. These exceptions, in addition to the observation of both high and low levels found within one single order (primates—Marroig and Cheverud 2001; Oliveira et al. submitted), reveal that the magnitude of integration can evolve considerably fast, and the possibility of large r^2 variation within diverse groups (e.g., rodents) cannot be discarded. A broader generalization, however, seems possible for metatherians, where high overall integration levels seem to be the rule: high r^2 values were found in all taxa examined in this study and also in a more detailed survey within Didelphimorphia (L. T. Shirai and G. Marroig, submitted). In short, the overall picture emerging from our broad scale comparisons of mammalian skulls is one of relative constancy of correlation and covariance patterns and, at the same time, a quite plastic magnitude of integration. Such plasticity might be an explanation for how the substantial diversity observed in the skull morphology of the mammal groups investigated could be produced even if the correlation/covariance patterns remained constant along their evolution (Fig. 4). If two groups have exactly the same inter-trait relationships, but differ significantly in the intensity of how these traits are connected (magnitude of integration), their response to evolutionary forces, like natural selection, could be strikingly different (Hansen and Houle 2008; Marroig et al. 2008). In general, groups with lower magnitudes respond more frequently in the direction of the selection gradients, while higher magnitudes are associated with lower evolvabilities. This issue was empirically addressed for the same taxa studied here, and is discussed in detail in a companion article (Marroig et al. 2008). Figure 4 also helps to understand this point. While both populations have the same correlation pattern is clear that population B with lower overall integration would respond more easily in most directions of the morphospace just because traits are not so tightly associated. In short, while mammalian skull diversity seems to have been produced by keeping relatively similar patterns of inter-trait covariance and modularity, changes in the magnitude of integration allow evolution in cranial trait averages without disrupting integration patterns.

Modularity

Modularity was assessed by comparing the correlation matrices of the sampled taxa with theoretical morphological integration matrices derived from hypotheses of developmental/functional relationships (Cheverud 1996; Marroig and Cheverud 2001). This approach was useful to test for the presence of cranial modules in the mammals orders studied.

All metatherians presented a similar modularity pattern. The five orders studied exhibited strong integration among the facial elements, especially in the oral and nasal sub-regions, and almost no integration in the neurocranium and its sub-regions (Table 5). In these taxa, the nasal and oral sub-regions were dominant modules, as detected by the ratio avg+/avg−, which is an index of the distinctiveness of the hypothesized modules (average = 1.47 and 1.43, respectively); moreover, these are the only evident modules in metatherians. These groups also presented the lowest values for the ratio avg+/avg− in the total integration hypothesis (average = 1.02), suggesting that their phenotypic modules are the least distinct among all studied mammals. Therefore, there is a striking contrast in these taxa between the high overall level of integration (r^2) and the low level of distinctiveness of each module. The explanation for this pattern may be related to an early development of the facial traits in this group, enabling a relatively less developed newborn to suckle in the pouch, where cranial development continues (Smith 1996). The precocious facial development probably imposes a constraint over the organogenesis of the remaining cranial structures, particularly the neurocranium, resulting in prominent faces in adults (Smith 1996, 1997). Such constraint is arguably strong, because newborn survival depends directly on its ability to suckle. In fact, this hypothesis may also explain why all metatherian groups exhibited very similar, and sometimes identical, morphological integration patterns.

Eutherians, in contrast, exhibited more variable modular patterns (Table 5), and most of the groups presented significant total and neuro-somatic integration. This modularity pattern represents the main difference in comparison with metatherians and agrees with what is known about the developmental history of eutherians. First of all, embryonic development is in fact more plastic in these mammals, resulting in a wider range of neonatal states when compared to metatherians (Smith 1997, 2001). Additionally, intra-uterine growth is relatively longer and suckling starts relatively later, so that the differentiation of the central nervous system can occur before the development of the bones and muscles of the head (Smith 1996). This sequence comparatively delays the development of the face and favors the emergence of neuro-somatic integration in eutherians. It is worth noting that these mammals also presented a relative reduction in overall integration magnitude (r^2), which is probably related to the reduction of the impact that size variation has over the total morphological variation (Fig. 3f). Groups with higher r^2 values tended to present size as the major source of variation in skull morphology, while groups with lower r^2 presented a much smaller size contribution to the total variation. In short, there seems to be a differential impact of growing on the development of each group, explaining the differences observed in the r^2 values and, therefore, the differences observed in the modular patterns.

Regarding the modularity patterns within eutherian orders, some deviations from the general trends are particularly interesting, and can be readily associated to the correlation/covariance structure analyses. Firstly, some eutherian orders have r^2 values comparable to those of metatherians (average = 0.32), like lagomorphs (0.19), and hyracoids (0.26). Contrary to other eutherians, these taxa presented a modular structure similar to those of metatherian groups, i.e., predominant facial integration and lack of total integration; therefore, in these cases the similarity in modularity patterns explains why the covariance structure of these distantly related groups was highly correlated. Secondly, only *Homo* and *Gorilla* matrices presented marked cranial vault integration. Considering that these two taxa are phylogenetically close and that both have relatively larger neurocrania with a proportionally larger brain, vault integration might be associated with highly developed brains in the primate lineage. In this context, *Pan* would be an exception, considering it has a comparably large neurocranium, but non-significant vault integration. However, the detection of integration in a given module by our approach depends on the magnitude of correlations in other modules. *Pan* shows extremely high oral and nasal integration (Table 5), a feature that might be masking an eventually high integration also in the cranial vault.

In our sample, *Homo* arguably revealed the most distinct modularity pattern. Not only it is one of the two taxa with significant vault integration, it is also the only one with neurocranial integration (Table 5). Besides, it has, by far, the highest avg+/avg− ratio in the total integration matrices, reflecting the presence of very apparent modules in the skull. Finally, *Homo* yielded the lowest r^2 value among all taxa sampled, indicating an overall poorly integrated (or parcellated) cranium. These trends can be readily seen in the plots of the avg+/avg− ratios against the r^2 levels for the oral and nasal sub-regions, as well as for the total integration and face hypotheses (Fig. 3). The distinctiveness of the morphological integration patterns of human skulls has already been detected in comparisons with other hominids (Ackermann 2005; Mitteroecker and

Bookstein 2008), but it is worth noting that Marroig and Cheverud (2001, Table 10) found that 5 out of 16 New World monkey genera also showed significant integration in the neurocranium. Regarding hominids, the departure from the general pattern observed in other primates seems to occur in the later stages of development, particularly in the neurocranium. It is not entirely clear why this might be so, although it indicates that selection was working in this lineage, either on humans or the apes, to distinguish them not only in morphology, but in integration patterning (Ackermann 2005). Considering that humans had a lower overall magnitude of integration in the cranium, it is possible that our species has been more responsive to natural selection than other hominids (Marroig et al. 2008), providing an explanation for its remarkable distinctiveness.

Among all taxa investigated in this study, *Homo* represents an extreme instance of low overall integration and high intra-module integration in the skull. Nevertheless, the positive and significant association between the phylogenetic history of mammals and the magnitude of the pairwise differences in r^2 between taxa indicates that the tendency towards a decrease in overall integration, and a simultaneous increase in the distinctiveness of the modules (avg+/avg− ratio), is valid for the whole phylogeny of mammals (Figs. 2 and 3). Although this finding may at first seem paradoxical, this parcellation pattern (sensu Wagner and Altenberg 1996) can be explained by a differential reduction in the level of correlations among traits within and between modules. If a more pronounced reduction occurred among traits in different modules, a decrease in the magnitude of overall integration would be expected, but the modules themselves would maintain, or even increase, their integration. Considering that phenotypic and genetic correlations can be thought as a consequence of pleiotropy (Marroig and Cheverud 2001), one possible explanation to this evolutionary trend is directional selection acting upon the epistatic variation in pleiotropy (Cheverud et al. 2004; Wagner et al. 2007; Pavlicev et al. 2008). It is important to note, however, that considerable variation in r^2 values might exist within orders, as already seen in primates (Marroig and Cheverud 2001).

Conclusions

Our data shed some light on several important aspects of the evolution of modularity in the mammalian skull. Firstly, the correlation/covariance structure of skull traits is, to a considerable degree, shared by all groups studied. Perhaps with the exceptions of *Homo*, *Gorilla* and *Pan*, morphological integration patterns are quite similar as demonstrated by the overall similarity among correlation and V/CV matrices. Also, judging from comparisons with a rodent genetic matrix, these similarities are not restricted to the phenotypic level and seem to extend to the underlying genetic matrices as well. This is a surprising result considering the large evolutionary timescale and diversity of taxa involved in our comparisons. Secondly, the similarity patterns were not associated to historical relatedness (phylogeny). Thirdly, morphological integration indexes exhibited great variation among groups. Taken together, these results suggest that while the modular structure could evolve at a slow pace in mammals, probably maintained by stabilizing selection due to functional and developmental constraints, the magnitude of integration and the degree of modularity itself might evolve considerably fast, in spite of the maintenance of the overall integration structure.

Another important finding relates to the differences in modularity patterns detected between more basal and more derived mammalian groups. Basal mammals exhibited higher *overall level* of integration (r^2) and lower *modular level* of integration (ratio avg+/avg−), while more derived mammals, like rodents and primates, showed the opposite pattern. Therefore, in a phylogenetic perspective, the history of the mammalian skull seems to be one of overall parcellation, while the modules themselves became relatively more integrated. A major evolutionary trend detected in the mammalian cranium has been a decrease in evolutionary constraints, brought about by increasing the modular architecture of the skull while simultaneously enhancing evolvability (see companion paper: Marroig et al. 2008).

Acknowledgements We thank Campbell Rolian and Katherine Willmore for the opportunity to present this data in the 2008 AAPA meeting. Benedikt Hallgrímsson and 2 anonymous referees made constructive comments on an earlier version of this paper. We are also grateful to the people and institutions that provided generous help and access to mammal collections: E. Westwig, N. Simmons, R. Voss and R. MacPhee (AMNH); L. Tomsett, P. Jenkins and D. Hills (BMNH); B. Paterson, W. Stanley, and L. Heaney (FMNH); J. Chupasko and M. Omura (MCZ); M. Godinot, F. Renoult, C. Lefrève and J. Cuisin (MNHN); L. Salles, J. Oliveira, F. Barbosa, and S. Franco (MNRJ); S. Costa and J. de Queiroz (MPEG); Staff at the Museo de la Universidad Nacional Mayor de San Marcos; M. de Vivo and J. Gualda (MZUSP); H. van Grouw and B. Bekkum-Ansari (Naturalis); R. Thorington, R. Chapman and L. Gordon (NMNH); M. Harman (Powell-Cotton Museum); Georges Lenglet (RBINS); E. Gilissen and W. Wendelen (RMCA); R. Asher, I. Thomas and D. Willborn (ZMB); F. Smith and S. Tardif (University of Tennessee, and the Oak Ridge Associated Universities Marmoset Research Center); C. Zollikofer, M. Ponce de Léon and T. Jashashvili (Zürich Universität); R. Smith (Museu de Anatomia da UNIFESP); E. Liberti (Museu de Anatomia "Professor Alfonso Bovero"). This research was supported by grants and fellowships from Fundação de Amparo à Pesquisa do Estado de São Paulo (FAPESP), Coordenação de Aperfeiçoamento de Pessoal do Ensino Superior (CAPES), Conselho Nacional de Pesquisas (CNPq), Fundação de Amparo à Pesquisa do Estado do Rio de Janeiro (FAPERJ), Fundação José Bonifácio (FUJB), Projeto de Conservação e Utilização Sustentável da Diversidade Biológica (PROBIO), and an American Museum of Natural History Collections Study Grant.

Appendix

Landmark abbreviations and definitions

Landmarks		
Abbreviations	Landmarks	Position
IS	Intradentale superior	Midline
PM	Premaxillary-maxillary suture at the alveolus	Both sides
NSL	Nasale	Midline
NA	Nasion	Midline
BR	Bregma	Both sides
PT	Pterion	Both sides
ZS	Zygomaxillare superior	Both sides
ZI	Zygomaxillare inferior	Both sides
MT	Maxillary tuberosity	Both sides
PNS	Posterior nasal spine	Midline
APET	Anterior petrous temporal	Both sides
BA	Basion	Midline
OPI	Opisthion	Midline
EAM	Anterior external auditory meatus	Both sides
PEAM	Posterior external auditory meatus	Both sides
ZYGO	Inferior zygo-temporal suture	Both sides
TSP	Temporo-spheno-parietal junction	Both sides
TS	Temporo-sphenoidal junction at petrous	Both sides
JP	Jugular process	Both sides
LD	Lambda	Midline
AS	Asterion	Both sides

References

Ackermann, R. R. (2005). Ontogenetic integration of the hominoid face. *Journal of Human Evolution, 48*, 175–197. doi:10.1016/j.jhevol.2004.11.001.

Ackermann, R. R., & Cheverud, J. M. (2000). Phenotypic covariance structure in tamarins (genus Saguinus): A comparison of variation patterns using matrix correlation and common principal component analysis. *American Journal of Physical Anthropology, 111*, 489–501. doi :10.1002/(SICI)1096-8644(200004)111:4<489::AID-AJPA5>3.0.CO;2-U.

Ackermann, R. R., & Cheverud, J. M. (2004). Morphological integration in primate evolution. In M. Pigliucci & K. Preston (Eds.), *Phenotypic integration: Studying the ecology and evolution of complex phenotypes* (pp. 302–319). Oxford: Oxford University Press.

Almasy, L., & Blangero, J. (1998). Multipoint quantitative trait linkage analysis in general pedigrees. *American Journal of Human Genetics, 62*, 1198–1211. doi:10.1086/301844.

Asher, R. J. (2007). A database of morphological characters and a combined-data reanalysis of placental mammal phylogeny. *BMC Evolutionary Biology, 7*, 108. doi:10.1186/1471-2148-7-108.

Beck, R. M. D., Bininda-Emonds, O. R. P., Cardillo, M., Liu, F.-G. R., & Purvis, A. (2006). A higher-level MRP supertree of placental mammals. *BMC Evolutionary Biology, 6*, 93.

Begin, M., & Roff, D. A. (2005). From micro- to macroevolution through quantitative genetic variation: Positive evidence from field crickets. *Journal of Evolutionary Biology, 58*(10), 2287–2304.

Beldade, P., & Brakefield, P. M. (2003). Concerted evolution and developmental integration in modular butterfly wing patterns. *Evolution & Development, 5*, 169–179. doi:10.1046/j.1525-142X.2003.03025.x.

Berg, R. L. (1960). The ecological significance of correlation pleiades. *Evolution; International Journal of Organic Evolution, 14*(2), 171–180. doi:10.2307/2405824.

Chernoff, B., & Magwene, P. M. (1999). Morphological integration: 40 Years later. In E. C. Olson & R. L. Miller (Eds.), *Morphological integration* (pp. 316–360). Chicago: University of Chicago Press.

Cheverud, J. M. (1982). Phenotypic genetic and environmental morphological integration in the cranium. *Evolution; International Journal of Organic Evolution, 36*(3), 499–516. doi:10.2307/2408096.

Cheverud, J. M. (1984). Quantitative genetics and developmental constraints on evolution by selection. *Journal of Theoretical Biology, 110*, 155–172. doi:10.1016/S0022-5193(84)80050-8.

Cheverud, J. M. (1988). A comparison of genetic and phenotypic correlations. *Evolution; International Journal of Organic Evolution, 42*, 958–968. doi:10.2307/2408911.

Cheverud, J. M. (1989). A comparative analysis of morphological variation patterns in the papionins. *Evolution; International Journal of Organic Evolution, 43*(8), 1737–1747. doi:10.2307/2409389.

Cheverud, J. M. (1995). Morphological integration in the saddle-back tamarin (*Saguinus fuscicollis*) cranium. *American Naturalist, 145*, 63–89. doi:10.1086/285728.

Cheverud, J. M. (1996). Developmental integration and the evolution of pleiotropy. *American Zoologist, 36*, 44–50.

Cheverud, J. M., Ehrich, T. H., Vaughn, T. T., Koreishi, S. F., Linsey, R. B., & Pletscher, L. S. (2004). Pleiotropic effects on mandibular morphology II: Differential epistasis and genetic variation in morphological integration. *Journal of Experimental Zoology Part B, 302*(5), 424–435. doi:10.1002/jez.b.21008.

Cheverud, J. M., & Marroig, G. (2007). Comparing covariance matrices: Random skewers method compared to the common principal components model. *Genetics and Molecular Biology, 30*(2), 461–469. doi:10.1590/S1415-47572007000300027.

Cheverud, J. M., Wagner, G., & Dow, M. M. (1989). Methods for the comparative analysis of variation patterns. *Systematic Zoology, 38*(3), 201–213. doi:10.2307/2992282.

De Conto, V. (2007). Genética quantitativa e evolução morfológica em Akodon cursor. PhD thesis, Universidade Federal do Rio de Janeiro, RJ.

Eble, G. (2004). The macroevolution of phenotypic integration. In M. Pigliucci & K. Preston (Eds.), *Phenotypic integration: Studying the ecology and evolution of complex phenotypes* (pp. 253–273). Oxford: Oxford University Press.

Ehrich, T., Vaughn, T. T., Koreishi, S. F., Linsey, R. B., Pletscher, L. S., & Cheverud, J. M. (2003). Pleiotropic effects on mandibular morphology I. Developmental morphological integration and differential dominance. *Journal of Experimental Zoology (Molecular and Developmental Evolution), 296B*, 58–79.

Falconer, D. S., & Mackay, T. F. C. (1996). *Introduction to quantitative genetics* (ed. 4). Harlow, Essex, UK: Longmans Green.

Gonzalez-Jose, R., van der Molen, S., Gonzalez-Perez, E., & Hernandez, M. (2004). Patterns of phenotypic covariation and correlation in modern humans as viewed from morphological integration. *American Journal of Physical Anthropology, 123*(1), 69–77. doi:10.1002/ajpa.10302.

Hansen, T. F., & Houle, D. (2008). Measuring and comparing evolvability and constraint in multivariate characters. *Journal of Evolutionary Biology, 21*(5), 1201–1219. doi:10.1111/j.1420-9101.2008.01573.x.

Helms, J. A., Cordero, D., & Tapadia, M. D. (2005). New insights into craniofacial morphogenesis. *Development, 132*, 851–861. doi:10.1242/dev.01705.

Kenney-Hunt, J. P., Wang, B., Norgard, E. A., Fawcett, G., Falk, D., Pletscher, L. S., et al. (2008). Pleiotropic patterns of quantitative trait loci for seventy murine skeletal traits. *Genetics, 178*, 2275–2288. doi:10.1534/genetics.107.084434.

Kitazoe, Y., Kishino, H., Waddell, P. J., Nakajima, N., Okabayashi, T., Watabe, T., et al. (2007). Robust time estimation reconciles views of the antiquity of placental mammals. *PLoS ONE, 2*, e384. doi:10.1371/journal.pone.0000384.

Klingenberg, C. P. (2004). Integration, modules and development: Molecules to morphology to evolution. In M. Pigliucci & K. Preston (Eds.), *Phenotypic integration: Studying the ecology and evolution of complex phenotypes* (pp. 213–230). Oxford: Oxford University Press.

Lande, R. (1979). Quantitative genetic analysis of multivariate evolution applied to brain: Body size allometry. *Evolution; International Journal of Organic Evolution, 33*, 402–416. doi:10.2307/2407630.

Marroig, G., & Cheverud, J. M. (2001). A comparison of phenotypic variation and covariation patterns and the role of phylogeny ecology and ontogeny during cranial evolution of New World monkeys. *Evolution; International Journal of Organic Evolution, 55*(12), 2576–2600.

Marroig, G., & Cheverud, J. M. (2005). Size as a line of least evolutionary resistance: Diet and adaptive morphological radiation in New World monkeys. *Evolution; International Journal of Organic Evolution, 59*, 1128–1142.

Marroig, G., et al. (2008). Companion paper.

Mitteroecker, P., & Bookstein, F. (2008). The evolutionary role of modularity and integration in the hominoid cranium. *Evolution; International Journal of Organic Evolution, 62*, 943–958. doi:10.1111/j.1558-5646.2008.00321.x.

Moore, W. J. (1981). *The mammalian skull*. Cambridge: Cambridge University Press.

Morriss-Kay, G. M. (2001). Derivation of the mammalian skull vault. *Journal of Anatomy, 199*, 143–151. doi:10.1017/S0021878201008093.

Murphy, W. J., Eizirik, E., Johnson, W. E., Zhang, Y. P., Ryder, O. A., & O'Brien, S. J. (2001). Molecular phylogenetics and the origins of placental mammals. *Nature, 409*, 614–618. doi:10.1038/35054550.

Oliveira, F. B., Porto, A., & Marroig, G. Similarity of phenotypic covariance and correlation patterns in the skull along the evolution of Old World Monkeys: A case for the G evolutionary stasis. (Submitted to the *Journal of Human Evolution*).

Olson, E. C., & Miller, R. L. (1958). *Morphological integration*. Chicago: University of Chicago Press.

Pavlicev, M., Kenney-Hunt, J. P., Norgard, E. A., Roseman, C. C., Wolf, J. J., & Cheverud, J. M. (2008). Genetic variation in pleiotropy: Differential epistasis as a source of variation in the allometric relationship between long bone lengths and body weight. *Evolution; International Journal of Organic Evolution, 62*(1), 199–213.

Preston, K. A., & Ackerly, D. D. (2004). Allometry and evolution in modular organisms. In M. Pigliucci & K. Preston (Eds.), *Phenotypic integration: Studying the ecology and evolution of complex phenotypes* (pp. 80–106). Oxford: Oxford University Press.

Revell, L., Harmon, L. J., Langerhans, R. B., & Kolbe, J. J. (2007). A phylogenetic approach to determining the importance of constraint on phenotypic evolution in the neotropical lizard, *Anolis cristatellus*. *Evolutionary Ecology Research, 9*, 261–282.

Roff, D. A. (1997). *Evolutionary quantitative genetics*. New York: Chapman and Hall.

Roff, D. A., & Mousseau, T. (2005). The evolution of the phenotypic covariance matrix: Evidence for selection and drift in *Melanoplus*. *Journal of Evolutionary Biology, 18*(4), 1104–1114. doi:10.1111/j.1420-9101.2005.00862.x.

Shirai, L. T., & Marroig, G. Evolutionary constraint and freedom: A comparison between New World marsupials and monkeys skull (submitted).

Smith, K. K. (1996). Integration of craniofacial structures during development in mammals. *American Zoologist, 36*, 70–79.

Smith, K. K. (1997). Comparative patterns of craniofacial development in Eutherian and Metatherian mammals. *Evolution; International Journal of Organic Evolution, 51*(5), 1663–1678. doi:10.2307/2411218.

Smith, K. K. (2001). The evolution of mammalian development. *Bulletin of the Museum of Comparative Zoology, 156*, 119–135.

Sneath, P. H., & Sokal, R. R. (1973). *Numerical taxonomy*. San Francisco: WH Freeman and Company.

Springer, M. S., Stanhope, M. J., Madsen, O., & de Jong, W. W. (2004). Molecules consolidate the placental mammal tree. *Trends in Ecology & Evolution, 19*(8), 430–438. doi:10.1016/j.tree.2004.05.006.

Steppan, S. J., Phillips, P. C., & Houle, D. (2002). Comparative quantitative genetics: Evolution of the G matrix. *Trends in Ecology & Evolution, 17*(7), 320–327. doi:10.1016/S0169-5347(02)02505-3.

Tapadia, M. D., Cordero, D. R., & Helms, J. A. (2005). It's all in your head: New insights into craniofacial development and deformation. *Journal of Anatomy, 207*, 461–477.

Wagner, G. P., & Altenberg, L. (1996). Complex adaptations and the evolution of evolvability. *Evolution; International Journal of Organic Evolution, 50*(3), 967–976. doi:10.2307/2410639.

Wagner, G. P., Kenney-Hunt, J. P., Pavlicev, M., Peck, J. R., Waxman, D., & Cheverud, J. M. (2008). Pleiotropic scaling of gene effects and the "Cost of Complexity". *Nature, 452*, 470–473. doi:10.1038/nature06756.

Wagner, G. P., Pavlicev, M., & Cheverud, J. M. (2007). The road to modularity. *Nature Reviews Genetics, 8*, 921–931. doi:10.1038/nrg2267.

Wible, J. R., Rougier, G. W., Novacek, M. J., & Asher, R. J. (2007). Cretaceous eutherians and Laurasian origin for placental mammals near the K/T boundary. *Nature, 447*, 1003–1006. doi:10.1038/nature05854.

Willis, J. H., Coyne, J. A., & Kirkpatrick, M. (1991). Can one predict the evolution of quantitative characters without genetics? *Evolution; International Journal of Organic Evolution, 45*(2), 441–444. doi:10.2307/2409678.

Wilson, D. E., & Reeder, D. M. (Eds.). (2005). *Mammal species of the world: A taxonomic and geographic reference*. Baltimore: Johns Hopkins University Press.

Young, R. L., & Badyaev, A. V. (2006). Evolutionary persistence of phenotypic integration: Influence of developmental and functional relationships on complex trait evolution. *Evolution; International Journal of Organic Evolution, 60*(6), 1291–1299.